NASA TECHNICAL MEMORANDUM


NASA TM X-3182

NASA TM X-3182

# AN EXPERIMENTAL INVESTIGATION OF COMPRESSOR STALL USING AN ON-LINE DISTORTION INDICATOR AND SIGNAL CONDITIONER

*William G. Costakis and Leon M. Wenzel*

*Lewis Research Center*

*Cleveland, Ohio 44135*


NATIONAL AERONAUTICS AND SPACE ADMINISTRATION • WASHINGTON, D. C. • APRIL 1975

# AN EXPERIMENTAL INVESTIGATION OF COMPRESSOR STALL USING AN ON-LINE DISTORTION INDICATOR AND SIGNAL CONDITIONER

by William G. Costakis and Leon M. Wenzel

Lewis Research Center

## SUMMARY

An experimental investigation was conducted to determine the relation of steady-state and dynamic distortion to engine parameters using a J85-13 turbojet engine. The steady-state and dynamic distortions were induced by a secondary-air jet system. A distortion indicator capable of computing two distortion indices was built and used in the testing. A special purpose automatic signal conditioning device was used as an interface between the distortion indicator and the transducer signals. This device was necessary because of the excessive drifting of the transducers. Steady-state results indicated good correlation between the two indices and stall margin. The results obtained using the two indices as instantaneous distortion indicators were not promising. The effect of turbulence on stall margin was also investigated, and a sensitivity factor was determined.

## INTRODUCTION

Recently, the effect of steady-state and dynamic distortion at the face of jet engine compressors has received considerable attention. A number of distortion indices have been used by jet engine manufacturers to correlate stall producing distortions and engine parameters (refs. 1 to 3).

A jet engine compressor under actual flight conditions experiences a combination of steady-state and dynamic distortions. Because dynamic distortion activity is believed to frequently combine in some manner with steady-state distortion to degrade compressor stall margin, a distortion index that can correlate both steady-state and dynamic distortion with compressor stall is of considerable importance.

Early attempts to correlate distortion with engine parameters were restricted to steady-state distortions because of the lack of good dynamic instrumentation. This

situation has improved in recent years, and a number of studies on dynamic distortion have been conducted (e.g., refs. 3 to 6). A primary goal of such studies is to develop an empirical distortion index that could be used both to catalogue the distortion generated by an inlet and to indicate the distortion tolerance for specific engines. Such an empirical procedure could be used to predict engine-inlet compatibility during inlet and engine development. In the design of advanced control systems, it would be of significant value to directly sense dynamic distortion. The inlet and engine controls could then be more closely integrated and distortion induced stalls thus minimized.

This report presents the implementation of two simple dynamic distortion indices with analog components suitable for on-line analysis. One index is new and is capable of calculating distortion levels for any shape and extent of distortion. The second is a well-known index used for steady-state distortion only in references 7 and 8.

The description and implementation of a signal conditioner designed and built for this test program is also presented. The signal conditioner was used as an interface between the dynamic pressure transducers and the distortion indicator. This device corrected zero offsets and sensitivity variations of the transducers either automatically or manually. The device, although built primarily for this test program, is versatile enough to be used in similar programs.

Steady-state and dynamic results using the two distortion indices are presented. A secondary-air jet system (reported in refs. 9 and 10) was used to create both the steady-state and dynamic inlet-pressure disturbances. To obtain dynamic distortion data, the total-pressure fluctuations were incrementally increased until compressor stall was encountered. Attempts to predict stall using the instantaneous values of the two indices, although not fruitful, are presented. A sensitivity of stall margin to average rms inlet total pressure activity is presented.

The test program was conducted in the propulsion systems laboratory altitude chamber at Lewis.

## SYMBOLS

A sensitivity drift factor

B zero offset drift factor

K transducer sensitivity $V/(N/cm^2)$

P compressor face total pressure, $N/cm^2$

$\overline{P}$ compressor face average total pressure, $N/cm^2$

R resistance, ohm

S logic level

t time

$\omega$ weighting factor

Subscripts:

f feedback

i input

j matrix column

k matrix row

min minimum value

V volts

$\alpha$ specific matrix column

$\beta$ specific matrix row

$60^{\circ}$ $60^{\circ}$ sector

## METHODS

One of the objectives of a total-pressure distortion index is to relate total-pressure distortions to the loss in compressor stall margin. The usefulness of the index depends on the degree of success in correlating distortion to the loss in stall margin. The elements used for index calculations usually are a combination of the magnitude and area of the low-pressure regions. The diversity of methods currently in use is indicative of the difficulty in adequately relating inlet distortion conditions with the corresponding effect on compressor behavior. Ideally, an infinite number of measurements would be used to describe inlet conditions. Practically, only a few measurements can be taken. For this particular test there were 36 dynamic total-pressure transducers at the face of the compressor. The transducer configuration is shown in figure 1.

The first index (DI1) requires that the pressure measuring transducers at the face of the compressor be equidistant. The hexagonal pattern of the compressor-face instrumentation (fig. 1) satisfied this requirement. First, an average pressure is computed from the 36 compressor-face pressures. A pressure difference between each station pressure and the average pressure is then established. The polarity of the station differential pressure establishes a logic level for each station. Stations with below average pressures are assigned a logic level of one, and stations with equal or above average pressures are assigned a logic level of zero.

From these station logic levels a weighting factor $\omega$ is determined for each station. The weighting factor of a station is the summation of all the logic levels adjacent to the station. The process of obtaining a weighting factor for each station is shown in figure 2. Figure 2(a) shows 10 of the 36 pressure measuring stations having pressures lower than average. Figure 2(b) shows the logic levels corresponding to figure 2(a). And figure 2(c) shows the station weighting factors corresponding to the logic levels of figure 2(b). Each pressure measuring station is assigned a weighting factor that indicates the stations relation to the low-pressure region.

If the pressure measuring stations are put in the grid pattern shown in figure 3, a mathematical expression for the weighting factor can be written:

$$\omega_{\alpha\beta} = -S_{\alpha\beta} + \sum_{j=\alpha-1}^{\alpha+1} \sum_{k=\beta-2}^{\beta+2} S_{jk} \tag{1}$$

where

$$S_{jk} = 1 \quad \text{for} \quad \Delta P_{jk} > 0$$

$$S_{jk} = 0 \quad \text{for} \quad \Delta P_{jk} \leq 0$$

$$\Delta P_{jk} = \overline{P} - P_{jk}$$

The product of the station differential pressure and their corresponding weighting factors are summed for all stations. The final summation is then divided by the average pressure $\overline{P}$ to obtain the distortion index DI1. The mathematical equation used to combine pressure and area to form the distortion index DI1 is

$$DI1 = \sum_{\alpha\beta}^{n} \frac{\omega_{\alpha\beta} \Delta P_{\alpha\beta}}{\overline{P}} \tag{2}$$

where

$$\Delta P_{\alpha\beta} = \overline{P} - P_{\alpha\beta} \quad \text{for} \quad P_{\alpha\beta} < \overline{P}$$

$$\Delta P_{\alpha\beta} = 0 \quad \text{for} \quad P_{\alpha\beta} \geq \overline{P}$$

The summation over all stations yields the distortion index DI1, which will be sensitive

to the size and depth of the distorted region. The simplicity of equations (1) and (2) allows straightforward implementation on either digital or analog computers. However, only an analog implementation is discussed in this report (presented in the appendix).

The second index presented in this report DI2, can be written mathematically as

$$DI2 = \frac{\overline{P} - P_{min,\,60^o}}{\overline{P}} \tag{3}$$

where $\overline{P}$ is the face average pressure and $P_{min,\,60^o}$ is the lowest circumferentially averaged pressure over a $60^o$ sector.

This index was used because the J85-GE-13 turbojet engine was sensitive to a $60^o$ critical angle of distortion (ref. 8). Figure 4 shows how the compressor-face instrumentation was divided into twelve $60^o$ areas of extent. Each hexagonal pattern of instrumentation represented $60^o$ of extent. Adjacent $60^o$ areas of extent overlapped each other by $30^o$. Each $60^o$ extent consists of seven pressure stations. The differential pressures of these seven stations are used to obtain the average differential pressure for each $60^o$ extent. The symbol $P_{min,\,60^o}$ denotes the pressure of the $60^o$ area extent with the lowest average pressure, and $\Delta P_{min,\,60^o}$ is its corresponding differential pressure. This index then becomes

$$DI2 = \frac{\Delta P_{min,\,60^o}}{\overline{P}} \tag{4}$$

where $\Delta P_{min,\,60^o} = \overline{P} - P_{min,\,60^o}$. Equation (4) is simple and can be used on either digital or analog computers. Herein the analog implementation is discussed as part of the distortion indicator (see the appendix).

## SIGNAL CONDITIONER

### Problem

One of the main obstacles in implementing these distortion indices was the excessive drift of the dynamic pressure transducer signals. All pressure signals received at the input of the distortion indicator should have the form

$$P_v = KP$$

where P is pressure in newtons per square centimeter measured by the transducer, $P_v$ is the voltage signal proportional to P, and K is the proportionality constant or total sensitivity. Actually, however, the signal received at the input of the indicator had the form

$$P_v = A(t)KP + B(t)$$

where A(t) and B(t) varied and drifted for each transducer signal. The drift of B(t) was considerable, but the drift of A(t) was, in general, small enough to be neglected. To implement these indices, it was necessary to use a device as an interface between the transducer signal and the distortion indicator to correct the offset B(t) and establish the same sensitivity A(t)K for all transducers. This device is hereinafter referred to as zespan. Because of the considerable drift of B(t), the signals had to be conditioned every 5 minutes.

## Method and Implementation

The methodology used in the designing of the zespan signal conditioning device is shown in figure 5. The differential pressure transducer, three-way valve, and reference pressure source represent, in a simplified fashion, the zero and span conditions required for the correction of the signal.

In the zero condition the differential pressure applied to the transducer is zero. This is accomplished by shunting the transducer so that the back pressure of the transducer is the same as the front. In the span condition the transducer must be subjected to a known differential pressure. This is accomplished by connecting the backside of the transducer to an accurate and well regulated pressure source.

During zero differential pressure, the voltage output of the transducer should be zero. Anything other than zero is a voltage offset, which must be corrected. The zespan procedure for correcting such voltage offsets is as follows: The reference voltage to the servoamplifier is set to zero. When the signal at the input of amplifier 1 (fig. 5) has a voltage offset, the output of the servoamplifier shows a voltage error. This voltage error drives motor 1, which in turn moves the wiper of potentiometer 1 to a position such that the output of amplifier 1 is zero. When the output of amplifier 1 is zero, the servoamplifier nulls and clears its command to motor 1 of potentiometer 1. The wiper of potentiometer 1 remains in this position until it is reset again as desired.

During the span condition, the voltage output of the transducer must be proportional to the differential pressure experienced by the transducer. The transducer voltage output per unit differential pressure is the transducer sensitivity. If the transducer

sensitivity is not the desired one, it can be corrected by the zespan as follows: The reference signal to the servoamplifier is set to the desired voltage proportional to P2 - $P_r$. If the output of amplifier 1 is not equal to the reference signal, the servoamplifier output shows an error. In this mode of operation the servoamplifier drives motor 2, which moves the wiper of potentiometer 2. When the wiper is moved to a position such that the output of amplifier 1 is equal to the reference, the servoamplifier nulls and clears its command to the motor of potentiometer 2. The wiper of potentiometer 2 remains in this position until it is reset again, as desired.

This zespan signal conditioner is capable of correcting up to 45 signals. The device may be operated manually or automatically for both zero and sensitivity corrections. In the manual mode both the selection and the correction of the signal may be performed without any restrictions on the order of selection. In the automatic mode all signals are selected and corrected in a predetermined order.

The schematic for the correction of one channel of signal is shown in figure 6. The correcting circuit performs the zero and span corrections on the input signal as required. There are 45 correcting circuits available in the unit. Selector 1 chooses the signal channel to be corrected either manually or automatically. In the automatic mode the signal used to step the selector wiper to the next channel is given by the servoamplifier after the correction of the previous channel has been completed. From the selector switch the signal is fed through a first-order filter with a corner frequency of 10 hertz. The filtered signal then is compared with the reference signal in the servoamplifier, and the correction is performed as previously described.

Selectors 2 and 3 select the zero and span potentiometers and the corresponding motors for each channel. These two selectors are synchronized with selector 1 in both the manual and automatic modes. Thus when a channel is selected for a zero or span correction, the corresponding potentiometer-motor combination is also selected. The zero or span mode of operation is selected with switch 1, and the channel is selected, as mentioned before, with selector 1.

In this test only 36 of the 45 zespan channels were used, since only 36 dynamic transducers were used.

## APPARATUS AND PROCEDURE

Tests were conducted on a J85-13 engine installed in an altitude chamber. A secondary-air jet system was installed in the engine inlet. A schematic diagram of the engine and inlet is shown in figure 7.

The secondary-air jet system consisted of 18 nozzles spaced over the inlet. The 18 nozzles were composed of six groups of three nozzles each; each group covered a

sextant of the inlet. The airflow from the jet nozzles opposed the primary airflow. The resultant momentum exchange effected a total-pressure loss across the jet nozzles.

Airflow to each group of three nozzles was controlled by a high response servovalve (ref. 9). The valves could be operated independently to achieve random or steady-state distortions. Figure 8 shows the frequency response of the secondary-air jet system. The ordinates are the amplitude ratio and phase shift of the average of the 36 inlet total pressures relative to the servovalve driving signal with all valves operating in unison. The resonant characteristics result from an impedance mismatch at the upstream end of the inlet duct.

The compressor face was instrumented with 36 total-pressure transducers arranged as was shown in figure 1. Miniature pressure transducers were used, mounted so as to provide a frequency-response essentially flat to 400 hertz.

Outputs from the 36 total-pressure transducers were recorded on a 42-channel FM tape recorder. Signals to drive the distortion valves were supplied from another tape recorder and were tailored on a desk-top analog computer.

In addition to the high response transducers, steady-state pressure taps were provided at each of the 36 inlet locations. These taps were connected to an accurate but slow data system (CADDE), which indicated steady-state pressures (ref. 11).

The 36 signals of the high-response transducers were fed into the zespan signal conditioner. The zespan corrected for zero offset and sensitivity error. The corrected total-pressure signals were then fed into the distortion indicator. The distortion indicator could be used to compute the two distortion indices during testing (on-line) or at a later time using signals recorded on the 42-channel tape recorder.

The accuracy of the zespan unit is better than 0.15 percent of full scale. The error expected from the distortion indicator does not exceed 3.5 percent of the output. These accuracies are based on simulated tests designed to determine the accuracy of both the zespan and the distortion indicator.

The procedure for testing was as follows: The test chamber pressure was adjusted so that the compressor-face pressure was 6.9 newtons per square centimeter. For steady-state testing the rotor speed was set at the desired value, and the exhaust nozzle adjusted such that the operating point lay below the surge line. Two methods were used to obtain steady-state distortion stalls. One method was to set the nozzle area for a turbine discharge temperature of 983 K and then increase the distortion amplitude until stall occurred. To obtain the desired steady-state distortion levels for a particular distortion pattern, the appropriate air jet valve discharge pressures were increased in a stepwise manner. The extent of distortion could be varied in increments of $60^{\circ}$. The other method of inducing steady-state distortion stalls consisted of setting a distortion level and then closing the nozzle area until stall occurred.

For the dynamic portion of the test, the rotor speed was set at the desired value, and the exhaust nozzle was adjusted so that the operating point be below the surge line.

The distortion valves were set to positions near midstroke to give the desired steady distortion, if any. The valves were then driven by six independent tracks of random noise that had been prerecorded on an FM tape recorder. These noise signals were operated on by an analog computer where their amplitudes could be set and their frequency content adjusted. The frequency content was adjusted by passing the noise signals through first-order filters. The corner frequency of the filters was set at 10, 50, or $\infty$ hertz (no filter), as required. The frequency content of the no-filter case was limited by the frequency response of the secondary-air jet system. The response of the secondary-air jet system was good to 100 hertz (fig. 8).

A test consisted of approximately 2 minutes of the noise signals driving the valves. If no stall occurred, the driving tape was rewound and played again at a higher amplitude. This was repeated until a compressor stall was induced.

## RESULTS AND DISCUSSION

Steady-state distortions were primarily induced by opening some of the distortion valves, which increased the airflow to the secondary-air jet system and, as a result, increased the valve discharge pressure. The valve discharge pressures to be increased were dictated by the extent and location of the desired distortion pattern. The remaining valves were kept at their lowest possible discharge pressure (13.8 $N/cm^2$), which corresponded to the valves' leakage flow.

Figures 9 and 10 show steady-state distortion levels indicated by the distortion indicator compared with the results obtained from the steady-state data system. Figure 9 shows the results obtained for the $60^\circ$, $120^\circ$, and $180^\circ$ distortion patterns. Figure 10 presents results obtained for the two $60^\circ$-per-revolution distortion patterns. The results obtained from DI2 index were close to the results from the steady-state data system. But the results from DI1 did not compare as well. The discrepancy is largely due to the sensitivity of the index to the small differences between the two measuring systems and pressure fluctuation. The dynamic transducers exhibited considerable drift as previously discussed. Before recording each data point, the dynamic transducer signals were corrected with the zespan signal conditioner. However, some drift still occurred during the testing. The drift causes the signals from the dynamic transducers to vary slightly from the corresponding steady-state data system signals. This small difference does not affect DI2 very much, but it will affect DI1 considerably. This is due to the logic in the evaluation of the weighting factor $\omega$, which makes DI1 very sensitive to small pressure changes. The logic levels required in the summation of $\omega$ can be either zero or one, depending on the polarity of the station signal with respect to the average total pressure $\overline{P}$. Dynamic transducer levels close to $\overline{P}$ may result in large

discrepancies between the on-line distortion indicator results and the steady-state data system results. Such discrepancies will occur when the magnitude of the dynamic signals is higher or lower than $\overline{P}$ while the magnitude of the corresponding steady-state data system signals is the opposite. Figures 9 and 10 give a good indication of the levels of distortion that were obtained from the secondary-air jet system. Small areas of extent tended to wash out more easily than larger areas. Also, at higher discharge pressures, the rate of change of distortion decreased as the discharge pressure increased. This, again, appears to be the result of mixing between the distorted and undistorted regions. The small diameter of the inlet may have been the cause of this problem. Distortion tests conducted using a large-diameter turbofan engine and a similar secondary-air jet system did not exhibit this problem at the levels of valve discharge pressures shown in this report (ref. 10).

The relation between steady-state distortion and stall margin loss is shown in figure 11. Stall margin loss is defined as the difference between the undistorted and the distorted stall pressure ratios at the same corrected speed. The data used in figure 11 were obtained by either holding the engine exhaust nozzle area constant and increasing distortion or by holding distortion constant and reducing the nozzle area until stall occurred. The data points are plotted without regard to the procedure that was followed. This was deliberate, since a distortion index should give good results independent of the procedure followed in obtaining the data. The extent of distortion used in obtaining these steady-state data was $180^{\circ}$ because higher levels of distortion could be obtained at this extent (as shown in figs. 9 and 10). The steady-state correlation between the two indices and stall margin loss, shown in figure 11, is very good. Two distinct boundaries defining the stall region for the 94 percent and 87 percent corrected engine speeds are clearly established. These results are in good agreement with the results presented in reference 8.

During the dynamic portion of the test, compressor stalls were induced by increasing the engine-face turbulence in a controlled manner. Three parameters were varied: the engine rotor speed, the frequency content of the signals driving the secondary-air jet system valves, and the amplitude of the superimposed steady-state distortion.

The rms amplitude of the pressure signals from six midannulus transducers (indicated by solid symbols in fig. 1) were measured for tests during which stalls occurred. The average of these six rms amplitudes are listed in table I for the various speeds, distortion amplitudes, and air jet frequencies considered.

The differential valve discharge pressure is the difference between the high and the low air jet discharge pressures, and hence is a measure of steady-state distortion. The values in table I do not show any consistent trends. However, if the values for 94-percent corrected speed are judged to be inconclusive because of insufficient data, a trend can be based on the results obtained for 87 percent corrected speed. For a corrected speed of 87 percent, the results for no filter and a 50-hertz corner frequency

filter show that the rms turbulence required to induce stall decreased as steady-state distortion increased. This trend was not evident in the results obtained with the 10-hertz filter. The results for the 87 percent corrected rotor speed are presented in figure 12.

An attempt to determine a correlation between the average rms turbulence and steady-state distortion indicated by the two indices is shown in figure 13. The index values plotted here were obtained using data from the steady-state data recording system and hence are a measure of steady-state distortion. Figure 13 does not show any reasonable correlation between average rms turbulence and steady-state distortion as indicated by the indices. The apparent lack of correlation between steady-state distortion and average rms turbulence may be due to the low levels of these characteristics achieved during the dynamic testing. Steady-state distortion during the steady-state testing was higher than the steady-state distortion during the dynamic testing for the same differential valve discharge pressure. The only difference between the two procedures was the level of the average secondary-air valve discharge pressure. For the dynamic testing the average pressure was considerably higher than for the steady-state testing. Again, demonstrating that as the average secondary-air valve discharge pressure increases, the mixing between distorted and undistorted regions also increases. The net result is a reduction in both the steady-state and dynamic distortions.

Figure 14 shows a transient recording of index DI2 before a typical stall. The hammer shock resulting from the stall and the distortion peak assumed to have caused the stall are indicated. Because of the lack of compressor interstage instrumentation, the peak assumed to have caused the stall was assumed to be the largest peak within 25 milliseconds before the hammer shock. Several peaks of equal or larger magnitude than the peak assumed to have caused the stall occur before stall. Both DI1 and DI2 exhibited this trend for all stall points obtained during this test. Both indices were passed through a first-order filter included in the distortion indicator. The filter time constant $\tau$ was 0.0005 second (1/8 rotor revolution). For some of the stall points DI1 and DI2 were also passed through additional first-order filters with time constants of 0.001, 0.002, and 0.004 second (1/4, 1/2, and 1 rotor revolution). The additional filtering did not improve the results. Figure 15 is a histogram of DI2 for approximately 22 seconds before stall for the same run as in figure 14. This histogram indicates that DI2 was greater than the peak assumed to have caused stall 5.1 percent of the time. This seems reasonably small. However, the frequency of occurrence of DI2 values equal to or greater than the stalling peak is too great to consider DI2 in a scheme to avoid stall. Figure 16 shows histograms of the stalling peak values of the two indices for the 18 stalls analyzed. The differences between the minimum and maximum values exceed 100 percent. The conclusion that can be derived from the results of figures 14 to 16 is that DI1 and DI2 do not appear to be good instantaneous indicators of stall.

Some insight into the relation between stall margin and turbulence can be gleaned from these tests. Figure 17 gives the amplitude of turbulence as a function of secondary flow and engine speed with no valve dynamic activity. The turbulence increases with secondary flow and engine speed. A limited amount of data were taken at 87 percent engine speed, but reasonable extrapolations can be made.

The effect the rms turbulence may have on stall margin is shown in table II. The first row for both the 87 and 94 percent correct rotor speed establishes the compressor pressure ratio for clean stall. It also establishes the rms turbulence with no secondary flow or valve dynamic activity. For the remaining data the operating points had a compressor pressure ratio 0.27 to 0.28 below the clean stall. When the turbulence at the inlet was increased by 0.074 to 0.080 newtons per square centimeter, stall occurred. This yields a turbulence to stall margin sensitivity factor of approximately 0.28 newton per square centimeter per unit of compressor pressure ratio.

## CONCLUDING REMARKS

An experimental investigation was made to determine the effect of steady-state and dynamic total-pressure distortion on a J85-GE-13 turbojet engine. Distortions were produced by a secondary-air jet system. A distortion indicator with the capability of computing two distortion indices was used to measure distortion. Also, a special purpose automatic signal conditioner was used as an interface between the transducers and the distortion indicator. The following conclusions can be made from the results of these tests.

1. A distortion indicator can be built with analog components whose size is small enough for flight, high altitude chamber, or wind tunnel testing. The quality of dynamic signals, even though greatly improved, still requires extensive conditioning before they are used by a distortion indicator.

2. The zespan signal conditioner is an automatic signal conditioner built primarily with analog components. The zespan is used to condition pressure signals before each data point. Both zero and sensitivity conditioning can be performed.

3. Index DI2 was better than DI1 throughout the test. When signals from small dynamic transducers are used, the variations in DI1 become large because of its sensitivity to pressure fluctuations.

4. Steady-state results indicated a good correlation between distortion and stall margin for both indices.

5. The dynamic results obtained using DI1 and DI2 as instantaneous distortion indicators were not promising. Distortion levels just before stall did not differ from distortion levels observed during the nonstall period of the same test. These indices can not be considered good instantaneous distortion indicators in a scheme to avoid stall.

6. Efforts to establish a correlation between average rms turbulence and steady-state distortion showed some promise but were not conclusive.

7. The effect of turbulence on stall margin was investigated for the two engine speeds examined in the test. A turbulence to stall margin sensitivity factor of approximately 0.28 newton per square centimeter per unit of compressor pressure ratio was found based on two operating points.

Lewis Research Center,
National Aeronautics and Space Administration,
Cleveland, Ohio, November 8, 1974,
505-05.

## APPENDIX - DI1 AND DI2 IMPLEMENTATION

The mathematical equation used to combine pressure and area to form the distortion index DI1 is as follows:

$$DI1 = \sum_{\alpha\beta}^{n} \frac{\omega_{\alpha\beta} \Delta P_{\alpha\beta}}{\overline{P}} \tag{2}$$

where

$$\Delta P_{\alpha\beta} = \overline{P} - P_{\alpha\beta} \quad \text{for} \quad P_{\alpha\beta} < \overline{P}$$

$$\Delta P_{\alpha\beta} = 0 \quad \text{for} \quad P_{\alpha\beta} \geq \overline{P}$$

The mathematical expression for the weighting factor $\omega_{\alpha\beta}$ is

$$\omega_{\alpha\beta} = -S_{\alpha\beta} + \sum_{j=\alpha-1}^{\alpha+1} \sum_{k=\beta-2}^{\beta+2} S_{jk} \tag{1}$$

where

$$S_{jk} = 1 \quad \text{for} \quad \Delta P_{jk} > 0$$

$$S_{jk} = 0 \quad \text{for} \quad \Delta P_{jk} \leq 0$$

where $\Delta P_{jk}$ is defined as

$$\Delta P_{jk} = \overline{P} - P_{jk}$$

These distortion indices DI1 and DI2 were implemented using analog computer components. The design of the analog computing unit for the calculation of the indices assumes that all station pressure level signals are positive voltages. The primary operations that must be made for DI1 are the calculations of the reference pressure, the station differential pressure, the logic level, and the weighting factor, the multiplication of station weighting factor by its differential pressure, and, finally, the summation of the products over all stations and its division by the reference pressure.

From the voltage signals representing station pressure levels, we compute a negative voltage proportional to the sum of all station pressures using summing amplifiers

as shown in figure 18. This circuit can average up to 45 signals. If less than 45 signals are to be averaged, the unused inputs of the circuit must be fed by the positive output signal proportional to the average of the inputs. In this particular test there were 36 pressure signals. Nine of the 45 inputs to the averaging circuit must be fed by $+\overline{P}$ as shown in figure 18.

The positive station voltage and the negative reference voltage are summed to form a voltage proportional to the differential pressure $\Delta P_{jk}$ of each station. This is done with a summing amplifier as shown in figure 19. For DI1 the output of the amplifier must be a positive voltage proportional to $\Delta P_{jk}$ for station pressures less than the reference pressure or a large negative voltage for station pressures larger than the reference pressure. To accomplish this, a limiter was used (fig. 19). In order for the limiter to be in the circuit, the switch must connect to the 15-volt source. When the switch is in the open position, the circuit is a simple summer. The logic level determination is based on the sign of the station differential-pressure amplifier output voltage. A positive voltage is required for a logic level of one; a negative voltage is required for a logic level of zero. The large negative voltage level is necessary to assure logic level control in the multiplication process.

The multiplication and station weighting factor summation is done by a single amplifier. This is possible since the logic level is either one or zero, which allows the multiplication to be an integral number of summations of the differential-pressure voltage. The circuitry for this operation is shown in figure 20. In this figure station 3, 7 is assumed to be the station whose product, $\Delta P_{3,7}\omega_{3,7}$ is desired. Stations 2, 6; 2, 8; 3, 5; 3, 9; 4, 6; and 4, 8 are the adjacent stations whose logic level determines the weighting factor $\omega_{3,7}$. The operation is based on the nonlinear characteristics of diodes 1 and 2. Diode 1 will pass negative voltage signals, and diode 2 will pass positive voltage signals. If station 3, 7 voltage is negative (station pressure higher than reference pressure), diode 2 will block all signals to the multiplication amplifier. The output of the amplifier then is zero, which satisfies the condition from equation (2) where, for $P_{jk} \geq \overline{P}$, $\Delta P = 0$. If the station 3, 7 signal is positive, it may or may not reach the multiplication amplifier, depending on the polarity of the signals coming from adjacent stations. If the adjacent station amplifier output voltages are positive (logic level of one), diode 1 will block them. For each block of adjacent station voltages, there is one $P_{3,7}$ voltage reaching the input to the amplifier. Therefore, for n number of adjacent stations with pressures less than reference, the output of the multiplication amplifier of this example will be $n\,\Delta P_{3,7}$. If the logic level of an adjacent station is zero, the output of their corresponding amplifiers is a large negative signal. This signal passes through diode 1 and overrides the signal from the station 3, 7 amplifier. Thus, a negative voltage appears at the input to diode 2, and no summation can occur. The station multiplication $\omega_{jk}\,\Delta P_{jk}$ is satisfied.

One amplifier can perform more than one station multiplication. For this configuration, six amplifiers performed two station multiplications each, and eight amplifiers performed three station multiplications each. The output of these amplifiers are summed, and the result is divided by the averaged signal to obtain the index as shown in figure 21.

The response of the amplifiers used in the calculation of DI1 is flat 10 kilohertz. The outputs of the reference signal and the $\sum \omega \Delta P$ were filtered. The corner frequency for the reference signal output was 4.6 hertz and for the $\sum \omega \Delta P$ was 300 hertz. The overall gain in the DI1 index was 0.0795 volt per unit weighting per volt difference between the reference and station signals. Provision for increasing this gain by factors of 2, 4, 10, and 20 are available.

The mathematical expression for DI2 is

$$DI2 = \frac{\Delta P_{min,\,60^o}}{\overline{P}} \tag{4}$$

where

$$\Delta P_{min,\,60^o} = \overline{P} - P_{min,\,60^o}$$

The primary operations for DI2 are the calculations of the average pressure $\overline{P}$, the differential pressure of each station with respect to the reference pressure $\Delta P_{jk}$, and the average differential pressure for each of the twelve $60^o$ areas of extent and the selection of the worst $60^o$ average differential pressure $\Delta P_{min,\,60^o}$. To obtain the final index, $\Delta P_{min,\,60^o}$ is divided by $\overline{P}$.

The circuitry used in the calculation of the reference pressure and the station differential pressures are the same ones used for DI1 (figs. 18 and 19). For this index, however, we are interested in pressures higher and lower than the average pressure. For this reason the limiter switch shown in figure 19 must be open. The station differential pressure amplifier then becomes a simple summer, whose output is proportional to both positive and negative differential pressures.

The $60^o$ area of extent pressure averaging circuit is shown in figure 22. The inputs to this circuit are differential pressure signals that are comprised in a $60^o$ area of extent or one hexagonal pattern. Twelve averaging circuits are needed to accommodate the twelve hexagonal patterns. The output of this circuit is a voltage proportional to the average differential pressure of its corresponding hexagonal pattern ($\Delta P_{60^o}$). The diodes at the input of this circuit are necessary to correct for the diode voltage drop of the previous circuit.

Figure 23 shows the circuit that selects the highest averaged differential pressure

of the 12 hexagonal patterns. The inputs to this circuit are the outputs of the 12 averaging amplifiers. In the diode configuration shown in figure 23, only positive voltage signals will conduct. At node b only the highest of the positive voltages will appear. This is true because the diodes fed by other than the highest positive signal will not conduct because of the negative voltage across these diodes. These diodes will conduct only when their corresponding input voltage signal becomes larger than the existing highest voltage signal. Diode 2 compensated for the voltage drop of the diode in diode group 1 that is conducting. The net voltage at point c then equals the highest input voltage at point a. The voltage signal at point c is fed into an amplifier and is then divided by $\overline{P}$ as shown. The output of the divider is KD2, where K is the total gain of the system.

Provision for the device to compensate for bad signals was available. When a pressure signal failed, three adjacent signals were averaged. This averaged signal then was used in place of the bad signal. The indicator could handle up to three bad signals in this fashion. The circuit for one substitute signal source is shown in figure 24.

## REFERENCES


1. Alford, Joseph S.: Inlet Flow Distortion Index. GER-1404, General Electric Co., 1957.

2. Oates, Gordon C.; Sherman, Dale A.; Motyclea, David L.: Experimental Study of Inlet-Generated Pressure Fluctuations. Presented at Airframe/Propulsion Comparability Symp., Air Force Aero Propulsion Lab., Air Force Flight Dynamics Lab., Wright Patterson AFB, June 1969.

3. Moore, M. T.: Distortion Data Analysis. General Electric Co. (AD-756481; AFADL-TP-72-111), 1973.

4. Burcham, Frank W., Jr.; Hughes, Donald L.; and Holtzman, Jon K.: Steady-State and Dynamic Pressure Phenomena in the Propulsion System of an F-111A Airplane. NASA TN D-7328, 1973.

5. Burstadt, Paul L.; and Calogeras, James E.: Instantaneous Distortion in a Mach 2.5 40-Percent-Internal-Contraction Inlet and Its Effect on Turbojet Stall Margin. NASA TM X-3002, 1974.

6. Costakis, William G.: Analog Computer Implementation of Four Instantaneous Distortion Indices. NASA TM X-2993, 1974.

7. Reid, C.: The Response of Axial Flow Compressors to Intake Flow Distortions. ASME Paper 69-GT-29, Mar. 1969.

8. Calogeras, James E.; Mehalik, Charles M.; and Burstadt, Paul L.: Experimental Investigation of the Effect of Screen-Induced Total-Pressure Distortion on Turbojet Stall Margin. NASA TM X-2239, 1971.

9. Baumbick, Robert J.: Device for Producing Dynamic Distortion Patterns at Inlets of Air-Breathing Engines. NASA TM X-2026, 1970.

10. Meyer, Carl L.; McAulay, John E.; and Biesadny, Thomas J.: Technique for Inducing Controlled Steady-State and Dynamic Inlet Pressure Disturbances for Jet Engine Tests. NASA TM X-1946, 1970.

11. Mealey, Charles; and Kee, Leslie: A Computer-Controlled Central Digital Data Acquisition System. NASA TN D-3904, 1967.

TABLE I. - COMPARISON OF TURBULENT DISTORTION

TO STEADY-STATE DISTORTION SHOWN AS

VALVE DISCHARGE PRESSURE

| Percent corrected speed | Filter corner frequency, Hz | Differential valve discharge pressure, $N/cm^2$ | | | |
|---|---|---|---|---|---|
| | | 0 | 6.9 | 13.8 | 20.7 |
| | | Turbulent distortion, rms | | | |
| 87 | ∞ | 0.132 | 0.121 | 0.113 | 0.109 |
| | 50 | 0.124 - 0.115 | .119 | .110 | .112 |
| | 10 | .129 | .130 | .134 | .133 |
| 94 | ∞ | .141 | ----- | .160 | .146 |
| | 50 | .154 | ----- | ----- | ----- |
| | 10 | .131 | ----- | ----- | ----- |

TABLE II. - EFFECT OF rms TURBULENCE ON STALL MARGIN

| Compressor pressure ratio | Secondary airflow | Secondary airflow valve discharge pressure, $N/cm^2$ | Valve dynamic activity | Turbulence, $N/cm^2$ rms | Stall |
|---|---|---|---|---|---|
| Corrected speed, 87 percent | | | | | |
| 5.41 | No | ---- | No | 0.046 | Yes |
| 5.13 | Yes | 41.4 | No | .103 | No |
| 5.13 | Yes | 41.4 | Yes | .122 | Yes |
| Corrected speed, 94 percent | | | | | |
| 6.74 | No | ---- | No | 0.066 | Yes |
| 6.47 | Yes | 41.4 | No | .121 | No |
| 6.47 | Yes | 41.4 | Yes | .146 | Yes |

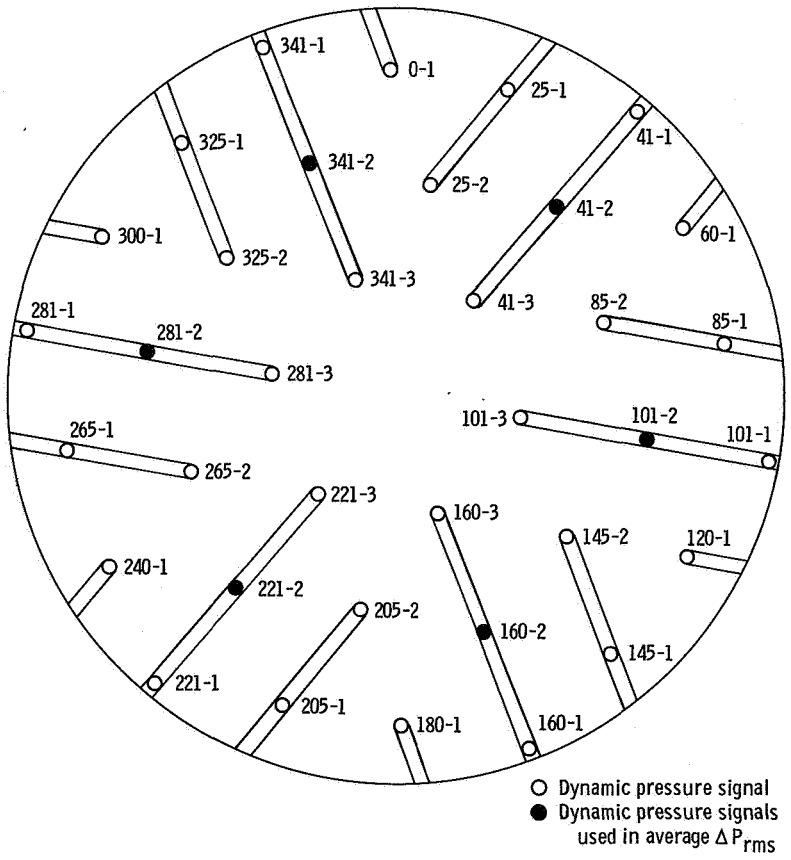


Figure 1. - Compressor-face total pressure instrumentation (looking upstream).

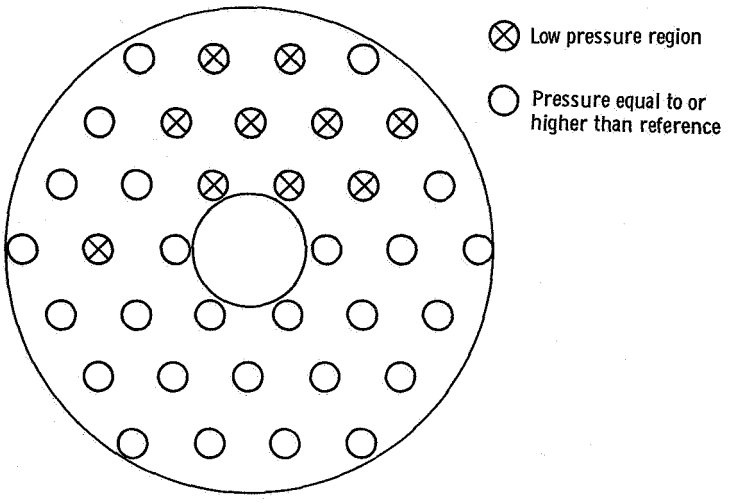


(a) Assumed pressure distortion.

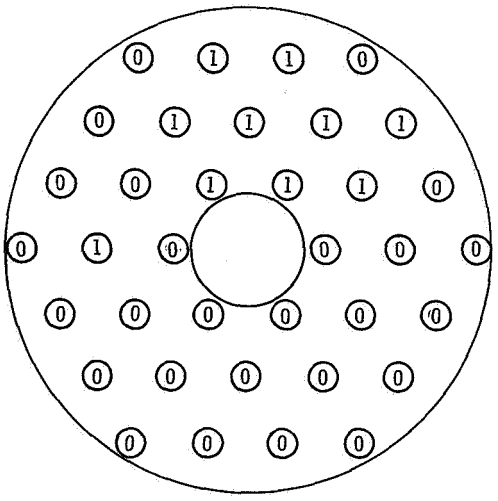

(b) Logic level for assumed pressure distortion shown in part (a).

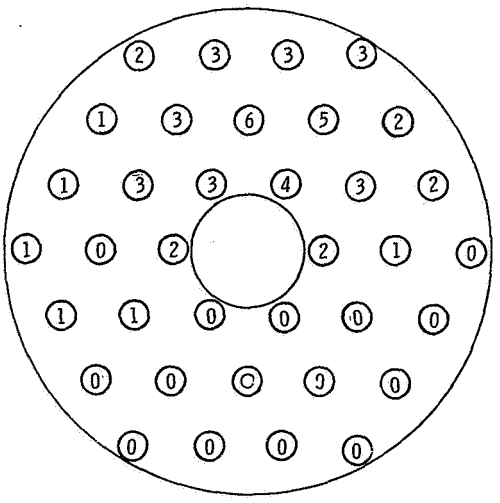

(c) Station weighting factors.

Figure 2. - Process of obtaining a weighting factor.

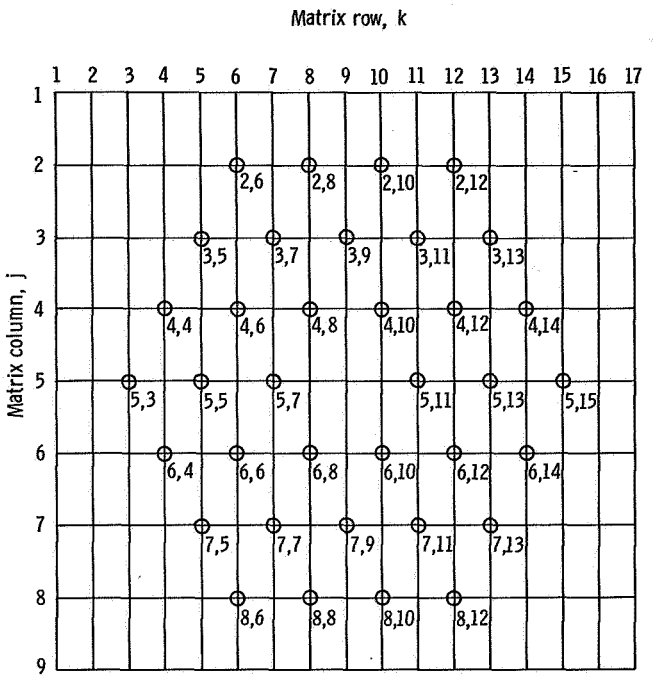


Figure 3. - Grid pattern for mathematical formulation.

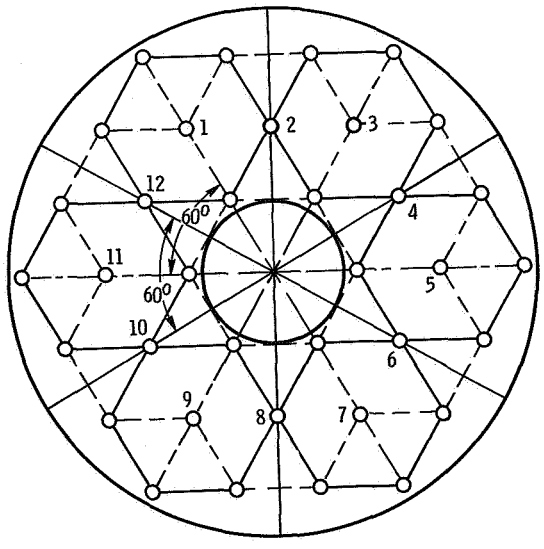


Figure 4. - Twelve $60^{0}$ segments as used for DI2.

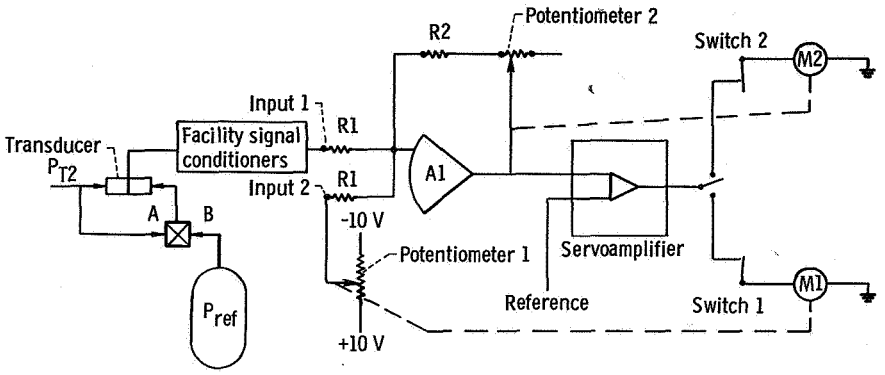


Figure 5. - Schematic of zespan circuitry.

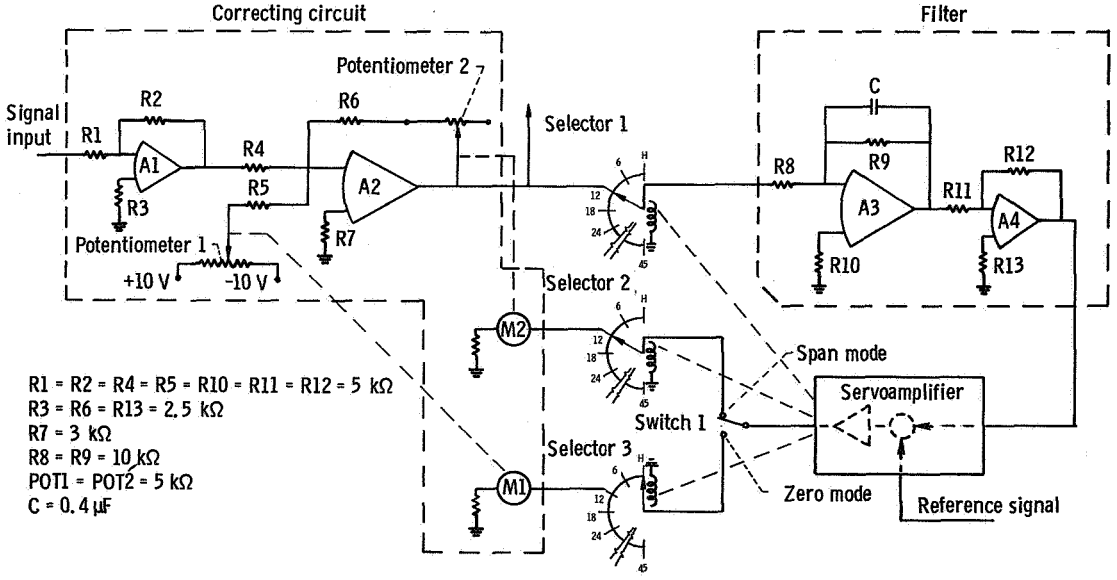


Figure 6. - Schematic showing zespan implementation.

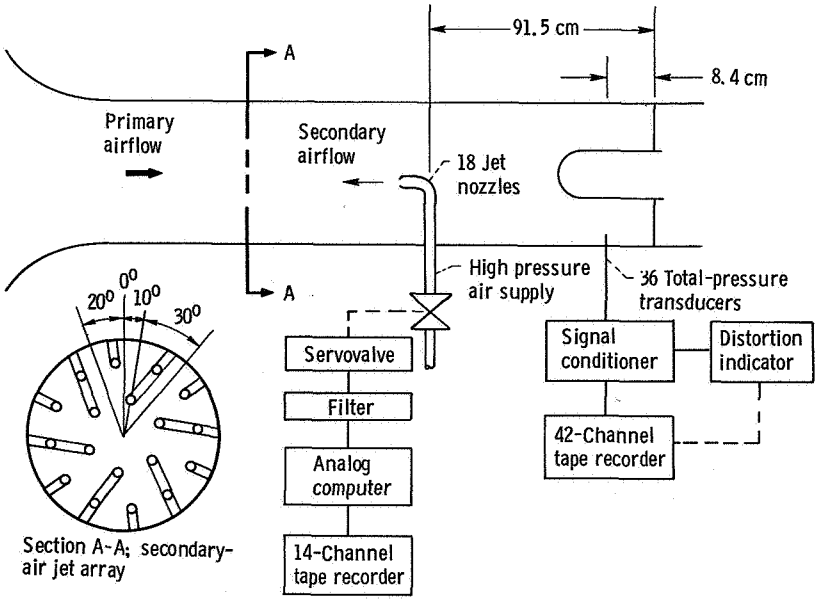


Figure 7. - J-85-13 Engine inlet with secondary jet system.

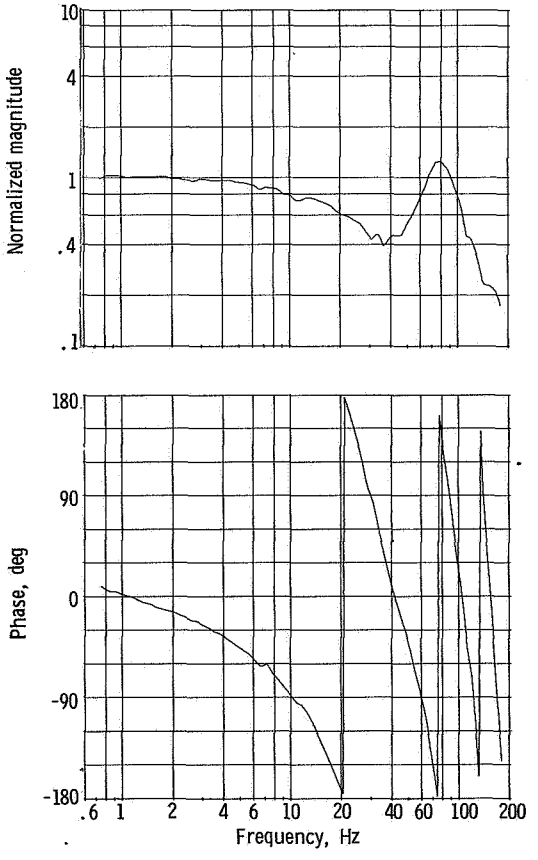


Figure 8. - Average inlet pressure perturbation relative to servovalve during signal.

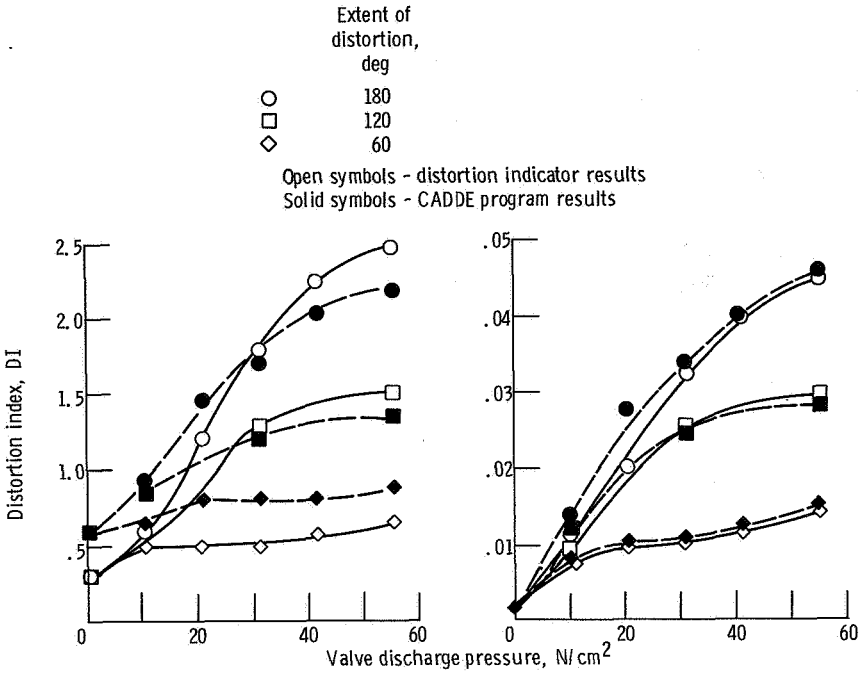


(a) Results for DI1. (b) Results for DI2.

Figure 9. - Comparison of distortion indicator results with CADDE program results.

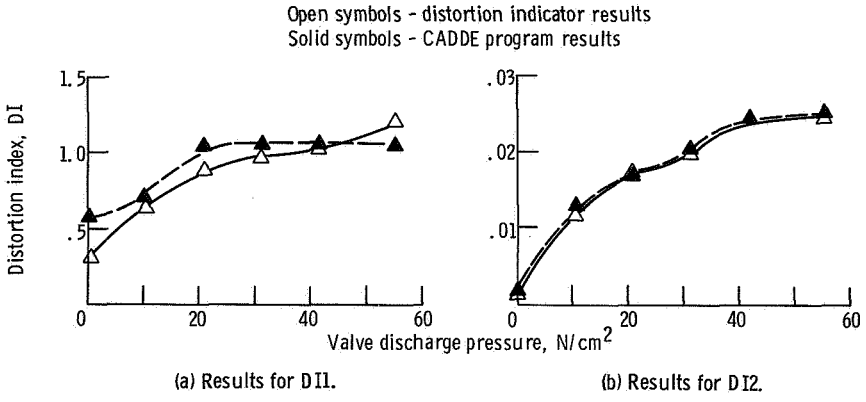


(a) Results for DI1. (b) Results for DI2.

Figure 10. - Comparison of distortion indicator results with CADDE program results for two $60^{0}$ per revolution distortion patterns.

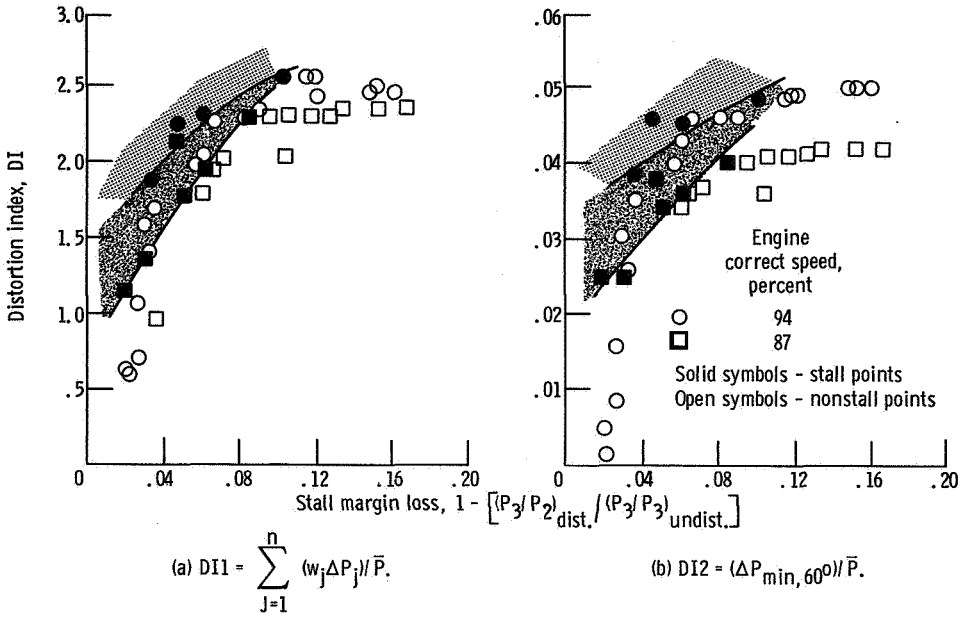


Figure 11. - Steady-state distortion as function of stall margin correlation for $180^0$ exent of distortion.

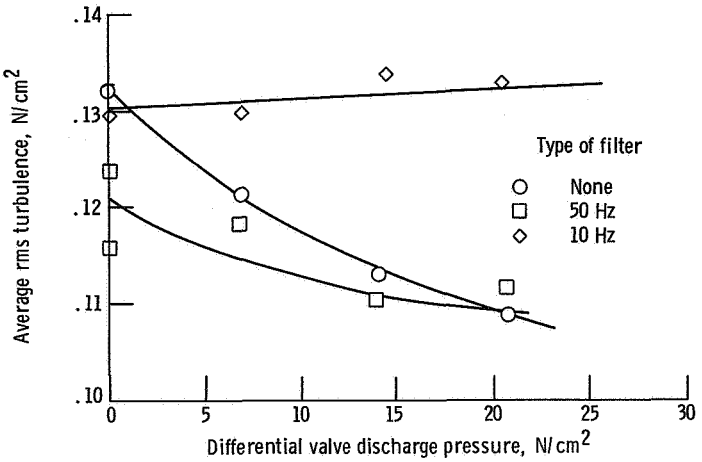


Figure 12. - Relationship between average turbulence rms and steady-state distortion at stall.

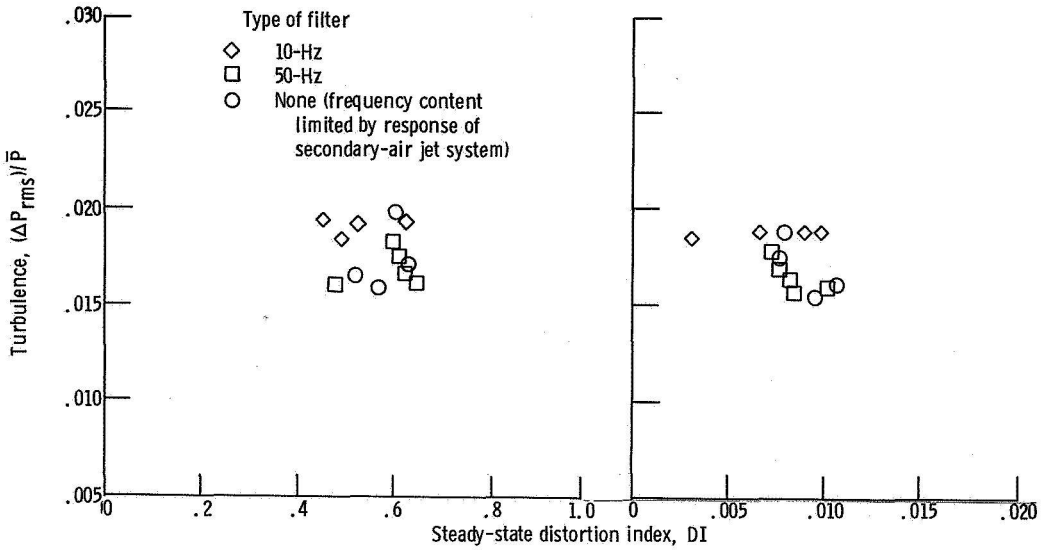


(a) Results for DI1. (b) Results for DI2.

Figure 13. - Rms inlet turbulence at stall as function of distortion indices, for 87 percent corrected rotor speed.

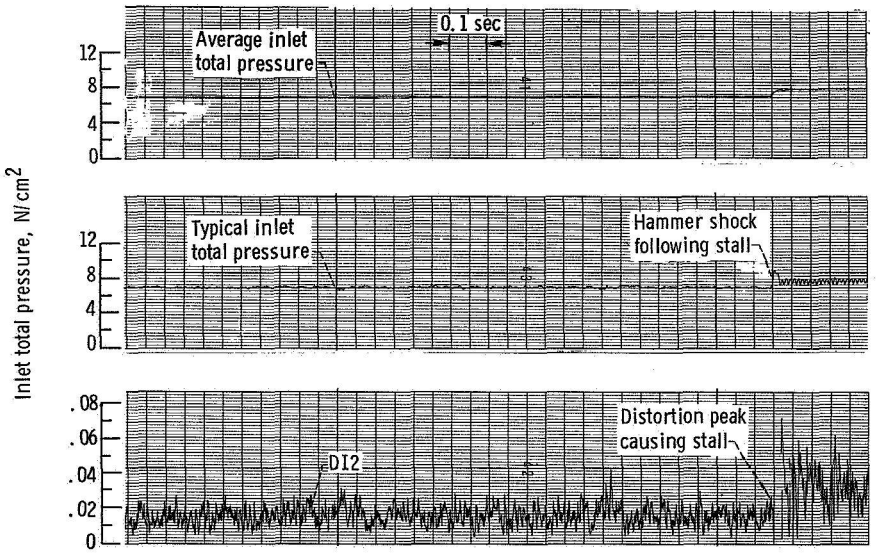


Figure 14. - Transient recording of inlet pressure and DI2 preceding typical stall.

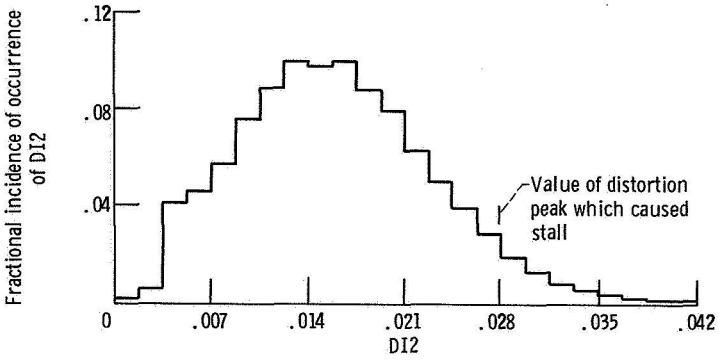


Figure 15. - Histogram of distortion index 2 (DI2) for typical stalling transient.

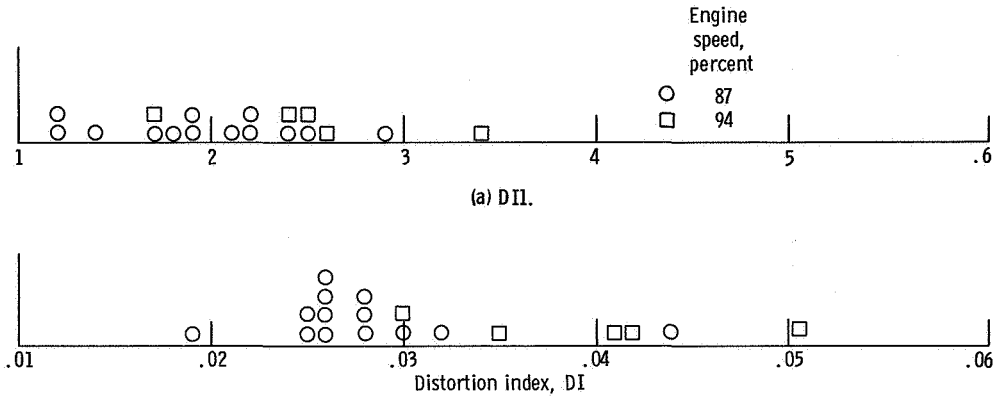


(a) DI1.

(b) DI2.

Figure 16. - Histograms of stalling peak values of indices for 18 stalls investigated.

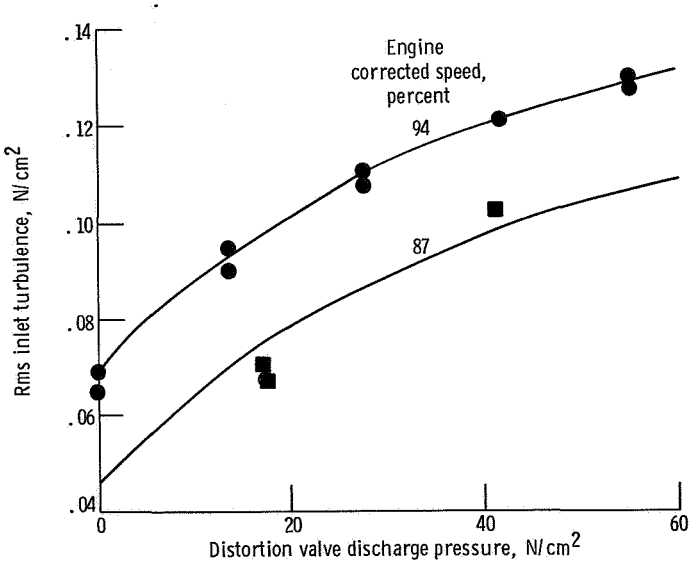


Figure 17. - Rms amplitude of background turbulence as function of secondary flow and engine speed.

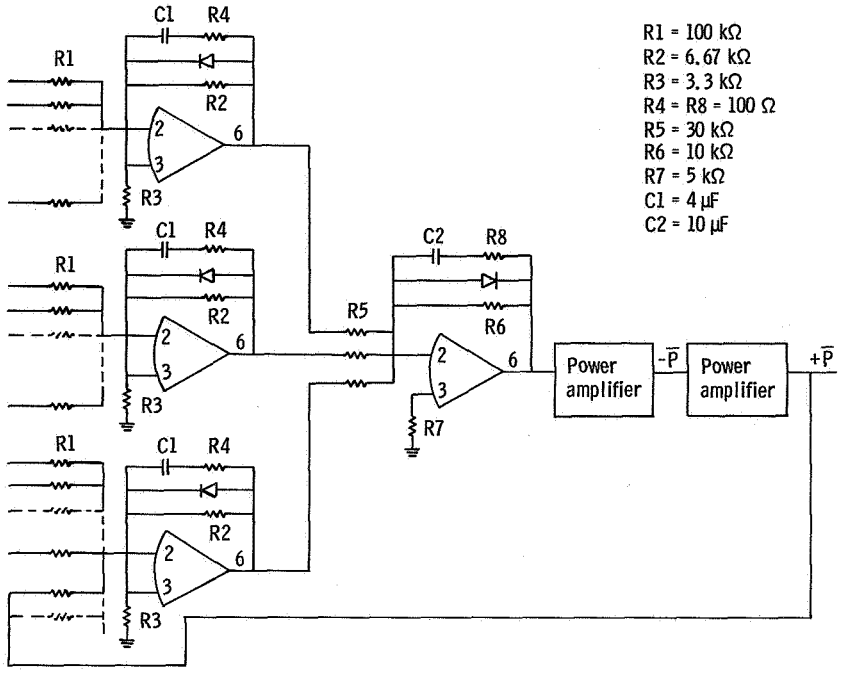


Figure 18. - Calculation of compressor-face average total pressure $\overline{P}$.

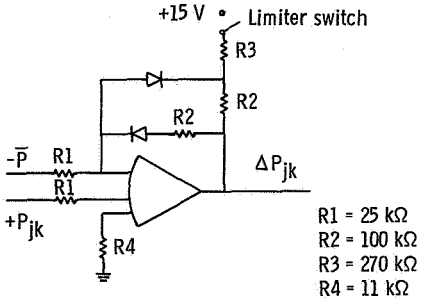


Figure 19. - Computation of station differential pressure

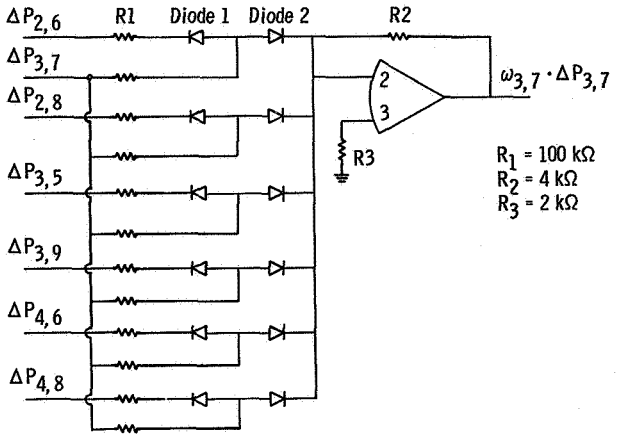


Figure 20. - Computation circuit for determining product of weighting factor and station differential pressure ($\omega \cdot \Delta P$).

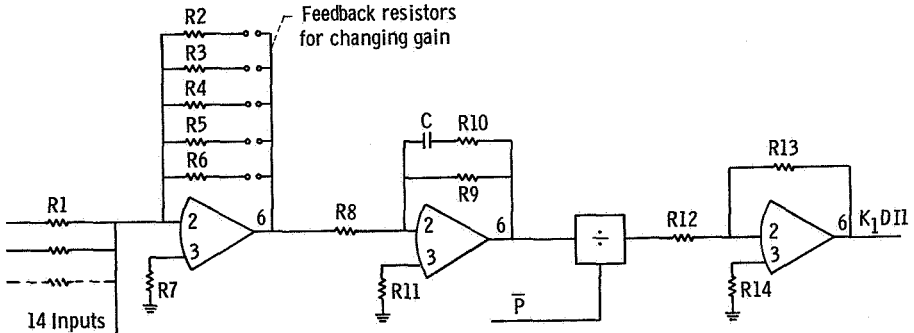


R1 = 100 kΩ
R2 = 100 kΩ
R3 = 50 kΩ
R4 = 20 kΩ
R5 = 10 kΩ
R6 = 5 kΩ
R7 = Variable
R8 = 10 kΩ
R9 = 10 kΩ
R10 = 100 kΩ
R11 = 5 kΩ
R12 = 10kΩ
R13 = 10kΩ
R14 = 5kΩ
C = 0.05μF

Figure 21. - Final summation and division by $\bar{P}$ to obtain index DI1.

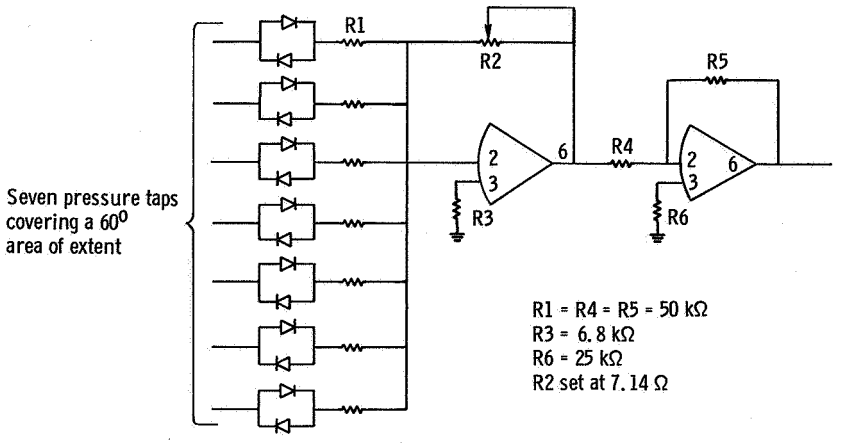


Figure 22. - 60° Area of extent averaging circuit.

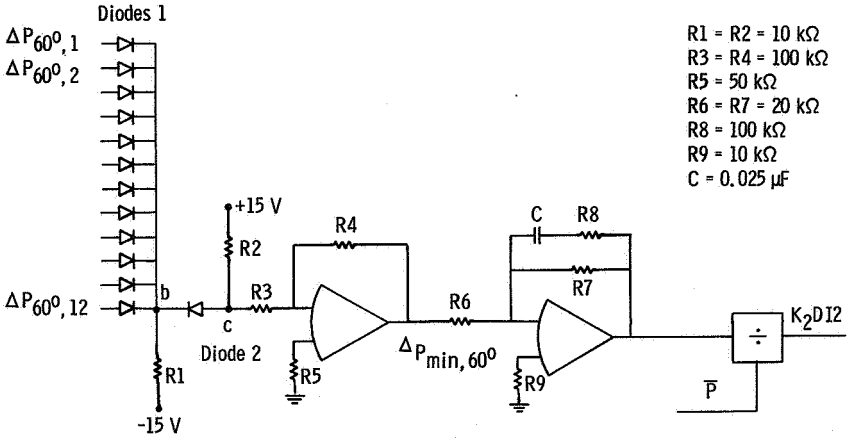


Figure 23. - High select circuit.

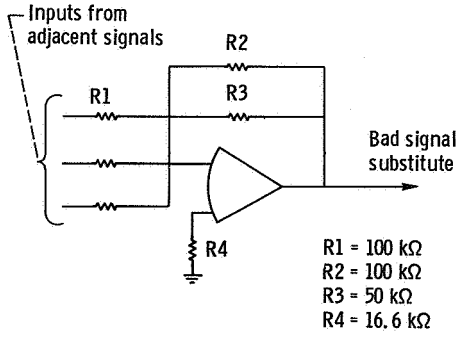


Figure 24. - Substitute signal circuit.

| 1. Report No. NASA TM X-3182 | 2. Government Accession No. | 3. Recipient's Catalog No. |
|---|---|---|
| 4. Title and Subtitle AN EXPERIMENTAL INVESTIGATION OF COMPRESSOR STALL USING AN ON-LINE DISTORTION INDICATOR AND SIGNAL CONDITIONER | | 5. Report Date April 1975<br>6. Performing Organization Code |
| 7. Author(s) William G. Costakis and Leon M. Wenzel | | 8. Performing Organization Report No. E-8120<br>10. Work Unit No. 505-05 |
| 9. Performing Organization Name and Address Lewis Research Center<br>National Aeronautics and Space Administration<br>Cleveland, Ohio 44135 | | 11. Contract or Grant No.<br>13. Type of Report and Period Covered Technical Memorandum |
| 12. Sponsoring Agency Name and Address National Aeronautics and Space Administration<br>Washington, D.C. 20546 | | 14. Sponsoring Agency Code |

15. Supplementary Notes

16. Abstract

The relation of the steady-state and dynamic distortions and the stall margin of a J85-13 turbojet engine was investigated. A distortion indicator capable of computing two distortion indices was used. A special purpose signal conditioner was also used as an interface between transducer signals and distortion indicator. A good correlation of steady-state distortion and stall margin was established. The prediction of stall by using the indices as instantaneous distortion indicators was not successful. A sensitivity factor that related the loss of stall margin to the turbulence level was found.

| 17. Key Words (Suggested by Author(s)) | 18. Distribution Statement |
|---|---|
| Distortion index<br>Dynamic distortion<br>Signal conditioner | Unclassified - unlimited<br>STAR category 01 (rev.) |

| 19. Security Classif. (of this report) | 20. Security Classif. (of this page) | 21. No. of Pages | 22. Price* |
|---|---|---|---|
| Unclassified | Unclassified | 32 | $3.25 |

* For sale by the National Technical Information Service, Springfield, Virginia 22151

NATIONAL AERONAUTICS AND SPACE ADMINISTRATION
WASHINGTON, D.C. 20546

OFFICIAL BUSINESS
PENALTY FOR PRIVATE USE $300

SPECIAL FOURTH-CLASS RATE BOOK

POSTAGE AND FEES PAID
NATIONAL AERONAUTICS AND SPACE ADMINISTRATION
451

POSTMASTER: If Undeliverable (Section 158 Postal Manual) Do Not Return

*"The aeronautical and space activities of the United States shall be conducted so as to contribute . . . to the expansion of human knowledge of phenomena in the atmosphere and space. The Administration shall provide for the widest practicable and appropriate dissemination of information concerning its activities and the results thereof."*

—NATIONAL AERONAUTICS AND SPACE ACT OF 1958

# NASA SCIENTIFIC AND TECHNICAL PUBLICATIONS

TECHNICAL REPORTS: Scientific and technical information considered important, complete, and a lasting contribution to existing knowledge.

TECHNICAL NOTES: Information less broad in scope but nevertheless of importance as a contribution to existing knowledge.

TECHNICAL MEMORANDUMS: Information receiving limited distribution because of preliminary data, security classification, or other reasons. Also includes conference proceedings with either limited or unlimited distribution.

CONTRACTOR REPORTS: Scientific and technical information generated under a NASA contract or grant and considered an important contribution to existing knowledge.

TECHNICAL TRANSLATIONS: Information published in a foreign language considered to merit NASA distribution in English.

SPECIAL PUBLICATIONS: Information derived from or of value to NASA activities. Publications include final reports of major projects, monographs, data compilations, handbooks, sourcebooks, and special bibliographies.

TECHNOLOGY UTILIZATION PUBLICATIONS: Information on technology used by NASA that may be of particular interest in commercial and other non-aerospace applications. Publications include Tech Briefs, Technology Utilization Reports and Technology Surveys.

***Details on the availability of these publications may be obtained from:***

**SCIENTIFIC AND TECHNICAL INFORMATION OFFICE**

**NATIONAL AERONAUTICS AND SPACE ADMINISTRATION**

**Washington, D.C. 20546**